COMMUNICATION

A sulphide lithium super ion conductor is superior to liquid ion conductors for use in rechargeable batteries†

Yoshikatsu Seino,*[a] Tsuyoshi Ota,[a] Kazunori Takada,[b] Akitoshi Hayashi[c] and Masahiro Tatsumisago[c]

We report that a heat-treated $Li_2S–P_2S_5$ glass-ceramic conductor has an extremely high ionic conductivity of 1.7×10^{-2} S cm^{-1} and the lowest conduction activation energy of 17 kJ mol^{-1} at room temperature among lithium-ion conductors reported to date. The optimum conditions of the heat treatment reduce the grain boundary resistance, and the influence of voids, to increase the Li$^+$ ionic conductivity of the solid electrolyte so that it is greater than the conductivities of liquid electrolytes, when the transport number of lithium ions in the inorganic electrolyte is unity.

Rechargeable Li-ion batteries have been widely used to power portable electronic devices in our information society, and could be installed in plug-in hybrid vehicles or smart grids in the near future.[1] However, the safety issues of Li-ion batteries that originate from combustible organic electrolytes are of greater concern with respect to vehicle or grid applications, because of the increased battery size. All-solid-state lithium secondary batteries with inorganic electrolytes are regarded as an ultimate solution to these safety issues.[2,3] However, solid-state lithium batteries have the disadvantage of low power density, because inorganic solid electrolytes, in general, have lower ionic conductivities than liquid electrolytes. Therefore, improvement of the ionic conductivity of the solid electrolytes is key to developing all-solid-state batteries for practical use.[4–9]

The power density of solid-state batteries has been limited by ion transport not only in the bulk, but also, at the grain boundary. It is well known that some oxide solid electrolytes show a high ionic conductivity of around 10^{-3} S cm^{-1}, but the grain boundary resistance is quite high to be rate-determining,

aIdemitsu Kosan Co. Ltd., Kami-izumi 1280, Sodegaura, Chiba, 299-0293, Japan. E-mail: yoshikatsu.seino@idemitsu.com; Tel: +81-438-75-7-24

bInternational Center for Materials Nanoarchitectonics, National Institute for Materials Science, 1-1 Namiki, Tsukuba, Ibaraki 305-0044, Japan

cDepartment of Applied Chemistry, Graduate School of Engineering, Osaka Prefecture University, 1-1 Gakuen-cho, Sakai, Osaka 599-8531, Japan

Broader context

Rechargeable Li-ion batteries are now widely used to power portable electronic devices and could be installed in plug-in hybrid vehicles or smart grids in the near future. The latter application is critical for establishing an environmentally-friendly society. However, safety issues, which originate from the use of combustible conventional organic electrolytes, are of greater concern in large batteries for vehicle or grid applications. It is anticipated that such safety issues could be addressed completely by using solid-state batteries, due to the non-flammability of solid electrolytes. Thus, inorganic solid electrolytes with high ionic conductivity are urgently required. We report an inorganic sulphide-based solid electrolyte that shows an extremely high ionic conductivity of 1.7×10^{-2} S cm^{-1}, by decreasing the grain boundary resistance, and the lowest conduction activation energy of 17 kJ mol^{-1} at room temperature among lithium-ion conductors reported to date. The optimum conditions of the heat treatment reduce the grain boundary resistance, and the influence of voids, to increase the Li$^+$ ionic conductivity of the solid electrolyte so that it is greater than the conductivities of liquid electrolytes, when the transport number of lithium ions in the inorganic electrolyte is unity.

even after high-temperature sintering. On the other hand, grain boundary resistance in sulphide solid electrolytes has been regarded as negligible; indeed, some sulphides show high ionic conductivities in the order of 10^{-3} S cm^{-1}, even in cold-pressed pellets without sintering. It has been generally considered that the grain boundary of the sulphide solid electrolyte does not contribute to its lithium ion conductivity. However, the grain boundary may affect ionic conduction in recently-developed sulphide solid electrolytes. For example, the ionic conductivity of the $Li_2S–P_2S_5$ glass-ceramic conductor was reported to be 3.2×10^{-3} S cm^{-1}, which is so high that the grain boundary resistance may no longer be negligible.

Here, we report that heat treatment gives the $Li_2S–P_2S_5$ glass-ceramic conductor an extremely high ionic conductivity of 1.7×10^{-2} S cm^{-1}, and the lowest conduction activation energy of 17 kJ mol^{-1} at room temperature among lithium-ion conductors reported to date. The optimum conditions of the heat treatment reduce the grain boundary resistance, and the influence of voids, to increase the Li$^+$ ionic conductivity of the solid

This journal is © The Royal Society of Chemistry 2014

Energy Environ. Sci., 2014, **7**, 627–631 | **627**

electrolyte so that it is greater than the conductivities of liquid electrolytes, when the transport number of lithium ions in the inorganic electrolyte is unity. We also discuss the relationship between the high ionic conductivity and the grain boundary resistance in the sulphide solid electrolytes.

The development of sulphide solid electrolytes began with studies on ion-conducting glass, and conductivities in the order of 10^{-3} S cm^{-1} had been observed only in sulphide glass in the 20th century. However, in the 21st century, such room-temperature conductivities also began to be achieved in crystalline materials. These conductivities were found in the Li$_2$S–GeS$_2$–P$_2$S$_5$ system called the thio-LISICON family, and in the Li$_2$S–P$_2$S$_5$ glass-ceramic system, with values of 2.2×10^{-3} S cm^{-1} and 3.2×10^{-3} S cm^{-1}, respectively. Subsequent studies initiated by these findings have resulted in the highest ionic conductivity in the Li$_2$S–GeS$_2$–P$_2$S$_5$ system, with a value of 1.2×10^{-2} S cm^{-1} for Li$_{10}$GeP$_2$S$_{12}$,[10] while that of the Li$_2$S–P$_2$S$_5$ glass-ceramic system remains in the order of 10^{-3} S cm^{-1}.

The activation energy (E_a) for conduction, calculated from the slope of an Arrhenius plot, is also an important parameter for evaluating ionic conduction, because it corresponds to the barrier height to ionic conduction. The E_a for Li$_{10}$GeP$_2$S$_{12}$ is reported to be 24 kJ mol^{-1}, while that for the 70Li$_2$S–30P$_2$S$_5$ glass-ceramic electrolyte with the highest conductivity in the glass-ceramic system, is 18 kJ mol^{-1}. Unexpectedly, the Li$_2$S–P$_2$S$_5$ glass-ceramic electrolyte has a lower ionic conductivity than Li$_{10}$GeP$_2$S$_{12}$, despite the lower barrier to ionic conduction.

An advantage of sulphide electrolytes, besides the high ionic conductivity, is the low grain boundary resistance. Although some oxide electrolytes show fast ionic conduction in bulk, the grain boundary resistance is too high to construct practical batteries.[11–13] On the other hand, the grain boundary resistance is believed to barely affect ionic conductivity in sulphide electrolytes. However, even a small grain boundary resistance may exert a large influence on the ionic conduction in the Li$_2$S–P$_2$S$_5$ glass ceramics to leave it of the order of 10^{-3} S cm^{-1} because of the high ionic conductivities. In this study, we investigated the influence of a heat treatment that unifies the electrolyte particles into a dense body free from grain boundaries, and found that the unification gives a Li$_2$S–P$_2$S$_5$ solid electrolyte with an extremely high ionic conductivity exceeding even those of liquid electrolytes.

In order to obtain the unified Li$_2$S–P$_2$S$_5$ glass-ceramic conductor, 70Li$_2$S·30P$_2$S$_5$ glass powder, which is pelletized at 94 MPa, is heated to just above the crystallization temperature (T_c). When the temperature exceeds the glass transition temperature, the heat treatment unifies the glass particles into a dense body, and further heating above the crystallization temperature crystallizes the glass into the glass-ceramic material.

The T_c was determined by differential scanning calorimetry (DSC), which shows the change in the specific heat corresponding to the glass transition at about 230 °C, as shown in Fig. S1 in the ESI.† The DSC curve also has a sharp exothermic peak due to crystallization at 255 °C (the onset point). As the exothermic crystallization ends at 280 °C, the heat treatment temperature was set at 280 °C or 300 °C. After the heat treatment, the glass phase is changed to a Li$_7$P$_3$S$_{11}$ crystal structure, as demonstrated in Fig. S2 in the ESI.†

The resulting sample is compared with the following two samples: cold-pressed Li$_2$S–P$_2$S$_5$ glass and the glass-ceramic material, i.e. samples that do not experience heat treatment after compression. The glass was synthesized by a rapid-quenching method, and it was transformed into the glass-ceramic material by heat treatment above the crystallization temperature (T_c) as described in ref. 14 and ref. 15.

Fig. 1 shows cross-sectional SEM images of the cold-pressed glass-ceramic (a), and the heat-treated pellet of the glass into the unified glass ceramic at 280 °C (b). The heat-treated pellet of the glass into the glass ceramic unifies the electrolyte particles into a bulk without grain boundaries, as shown in the SEM image (b).

Since the densification process highly unifies the glass-ceramic particles into a dense pellet, the individual grains and the grain boundaries are hardly seen, whereas they are still recognizable in the cold-pressed glass-ceramic material.

Fig. 2 shows the temperature dependency of the electrical conductivities of the 70Li$_2$S·30P$_2$S$_5$ samples. The ionic conductivities at 25 °C of the cold-pressed 70Li$_2$S·30P$_2$S$_5$ glass and glass-ceramic material are 8.0×10^{-5} S cm^{-1} and 1.4×10^{-3} S cm^{-1}, respectively. This difference is attributable to precipitation of Li$_7$P$_3$S$_{11}$ crystals with high ionic conductivity by heat treatment at 280 °C, which transforms the glass into the glass-ceramic material. On the other hand, unifying the glass-ceramic material by heat treatment at 280 °C increases the ionic conductivity to 1.7×10^{-2} S cm^{-1}. This conductivity is five-times higher than that previously observed in the Li$_2$S–P$_2$S$_5$ system[14] and even exceeds that of the recently-reported electrolyte, Li$_{10}$GeP$_2$S$_{12}$.[10]

Although grain boundary resistance has been regarded as being too small to observe in sulphide solid electrolytes, the high ionic conductivity in the bulk of these sulphides has revealed the grain boundary resistance. Nyquist plots show two semicircles when the impedances are measured at −35 °C, as shown in Fig. 1(c) and (d). Such semicircles observed for solid electrolytes in high and low frequency regions are due to bulk and grain boundary responses, respectively.

The impedance spectra are clearly separated into two semicircles only at low temperatures. When the temperature increases from −35 °C, the semicircle observed at low frequencies for the densified glass-ceramic material disappears from the Nyquist plot immediately.

The disappearance of the semicircle suggests the negligible contribution of the grain boundary to the total resistance in the unified glass-ceramic material in the given temperature range, which can be expected from the indistinguishable grain boundaries in the SEM image. On the other hand, the semicircle in the low frequency region for the cold-pressed sample persists up to room temperature.

Fig. 3 shows the temperature dependency of the bulk and grain boundary contributions in the cold-pressed glass-ceramic material below room temperature. The activation energies (E_a) for the bulk and grain boundary contributions, calculated by fitting the data to the Arrhenius equation, are 28 kJ mol^{-1} and

628 | Energy Environ. Sci., 2014, 7, 627–631

This journal is © The Royal Society of Chemistry 2014
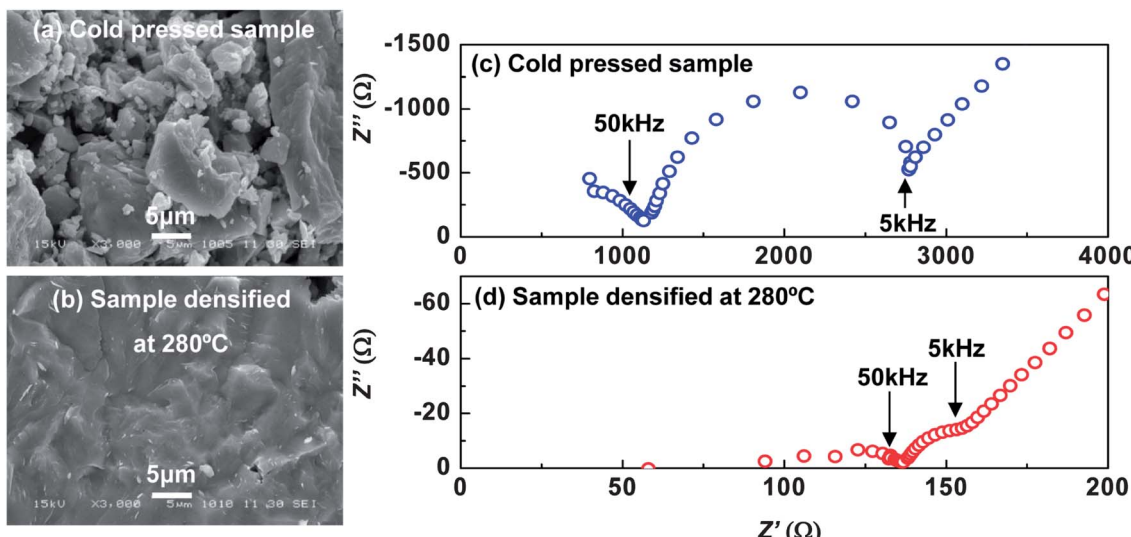
Fig. 1 SEM images of the 70Li$_2$S·30P$_2$S$_5$ glass–ceramic material from a cold-pressed sample (a) and the heat-treated sample at 280 °C (b). Complex impedance plots at −35 °C for the 70Li$_2$S·30P$_2$S$_5$ glass–ceramic material after cold pressing (c) and heat treatment at 280 °C (d).
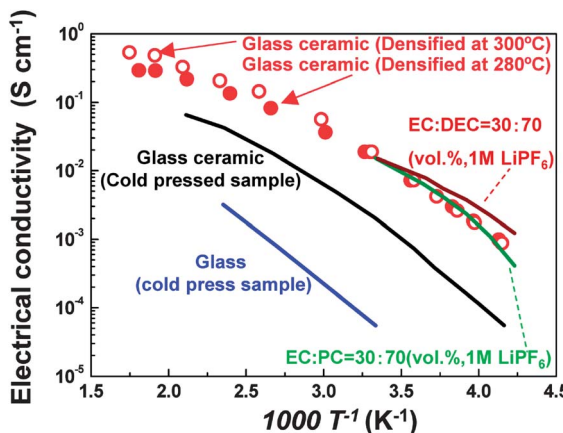
Fig. 2 Temperature dependency of the electrical conductivities of the 70Li$_2$S·30P$_2$S$_5$ glass–ceramic samples unified at 280 °C and 300 °C. The electrical conductivities of the cold-pressed glass and glass-ceramic powders, and of some typical liquid electrolytes (1 M LiPF$_6$ in EC–DEC and 1 M LiPF$_6$ in EC–PC) are also shown for comparison purposes.
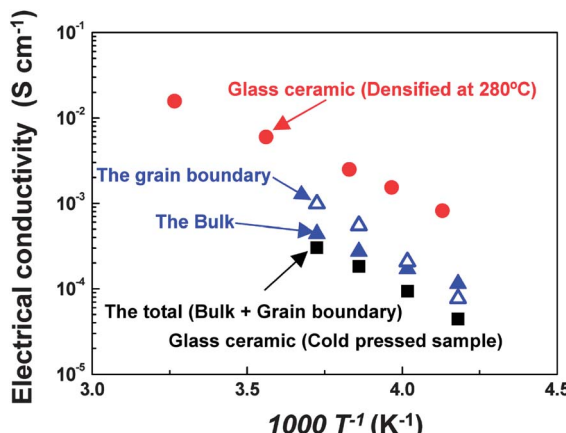

Fig. 3 Temperature dependency of the bulk and grain boundary resistances of the cold-pressed glass-ceramic material. The bulk and grain boundary resistances are conveniently converted into the corresponding conductivities by Ohm's law, in order to assess and compare the temperature dependency of the total conductivities of the cold-pressed and unified glass-ceramic materials.

48.5 kJ mol^{-1}, respectively. The figure also shows the electrical conductivities, i.e. overall conductivities including the bulk and grain boundary contributions, of the cold-pressed and unified glass-ceramic samples. The E_a for the densified glass-ceramic material below room temperature is 26 kJ mol^{-1}, which agrees well with the E_a for the bulk response in the cold-pressed material in the corresponding temperature range.

This agreement suggests that the densification process increases overall conductivity, not by enhancing ionic conduction in the bulk, but by reducing the grain boundary resistance. On the other hand, the grain boundary response in the cold-pressed glass-ceramic material is still apparent at up to 25 °C, which increases the E_a for the overall conductivity to 38.5 kJ mol^{-1}.

It should be noted that there is a significant difference in the conductivity between the before-unified and the after-unified materials, even in the high temperature region, where the influence of the grain boundary on the conductivity seems very small. One of the reasons is the low packing density in the non-unified material. It has many pores, as shown in Fig. 1(a), which decrease the cross section for ionic conduction. In effect, it can be concluded that the extremely high ionic conductivity of the unified glass-ceramic material is achieved by its low porosity as well as a decreased grain boundary resistance resulting from heat treatment. Fig. 4 shows the first cyclic voltammogram of the unified glass-ceramic material. Lithium deposition (Li$^+$ + e$^-$ → Li) and dissolution (Li → Li$^+$ + e$^-$) reactions are observed as redox waves at around 0 V vs. Li/Li$^+$ in the voltammogram. The
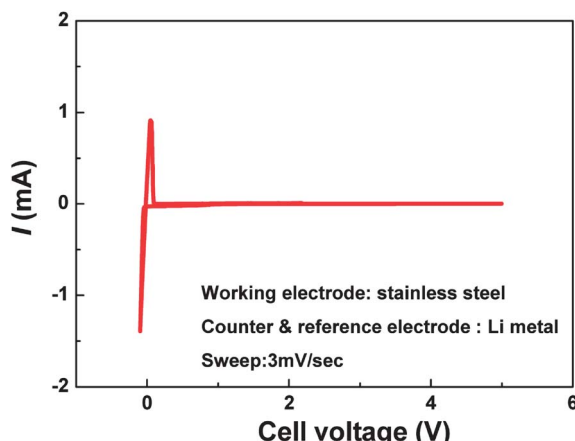
Fig. 4 Cyclic voltammogram of the $70Li_2S \cdot 30P_2S_5$ glass-ceramic electrolyte after heat treatment at 280 °C for 2 h. The voltammogram was obtained at room temperature at a scanning rate of 3 mV s^{-1}.

coulombic efficiency in the reactions is almost unity, which guarantees the stability of the lithium metal. Moreover, the voltammogram does not show any other reaction apart from lithium deposition and resolution in the potential range from −0.1 to 5 V vs. Li/Li$^+$. Although a conceivable decomposition reaction in sulphides is the oxidation of sulphide ions, they are immobile in solids and thus never diffuse to the electrode surface to be oxidized.[3,9,10] Therefore, the $70Li_2S \cdot 30P_2S_5$ glass-ceramic electrolyte has a wide electrochemical window, similar to many sulphide solid electrolytes.

The $70Li_2S \cdot 30P_2S_5$ glass-ceramic electrolyte in this study shows high ionic conductivity through the unification of the electrolyte particles into a dense electrolyte layer that reduces the grain boundary resistance and which precipitates highly-conductive crystals. The conductivity is one order of magnitude greater than the highest one previously observed with respect to the glass-ceramic system, reaching 10^{-3} S cm^{-1} even at a low temperature of −35 °C, owing to the low E_a of 17 kJ mol^{-1}. The conductivity is not only the highest among all lithium ion conductors reported to date, but is also as high as that of any non-aqueous electrolyte. Fig. 2 includes conductivity data for 1 M LiPF$_6$ in ethylene carbonate–diethyl carbonate (EC–DEC) and ethylene carbonate–propylene carbonate (EC–PC), which are usually used as liquid electrolytes in commercial lithium-ion batteries, for comparison purposes. The room temperature conductivities are 2.0×10^{-2} and 1.7×10^{-2} S cm^{-1}, respectively. Although these values are comparable to that observed in the present unified glass-ceramic material, the Li$^+$ ion transport number of the liquid electrolyte is around 0.5.[16,17] On the other hand, the Li$^+$ ion transport number of the inorganic electrolytes is unity, and thus it can be concluded that the unified glass-ceramic material has a higher lithium-ion conductivity than those liquid electrolytes.

These results demonstrate that the sulphide inorganic solid electrolytes have superior properties for battery applications to organic liquid electrolytes, which are currently used in commercial batteries. Thus, these glass-ceramic materials are good candidates for use as solid electrolytes for all-solid-state secondary batteries. In fact, graphite in this unified solid electrolyte exhibits a higher performance than in a non-unified electrolyte, as demonstrated in Fig. S3 and S4 in ESI.† The unified glass-ceramic material decreases the cell resistance and increases discharge capacity from the graphite electrode. However, we have to overcome a problem in the cathode interface to exploit the high potential of the electrolyte for use in solid-state batteries. The heat treatment to unify the glass-ceramic material promotes a reaction between it and the oxide cathode in the unification process, increasing the interfacial resistance. Suppression of this reaction is our next challenge to realize high-performance solid-state batteries, and is currently in progress.

Experimental section

The $70P_2S_5$–$30Li_2S$ glass was synthesized from reagent-grade chemicals, P_2S_5 (Aldrich, 99%) and Li_2S (Idemitsu, 99%). A mixture of these chemicals was sealed in a carbon-coated quartz tube and heated at 700 °C for 2 h in an electric furnace. The molten sample was rapidly quenched in ice water. The glass-ceramic material for the cold-pressed sample was prepared by heat treatment of the obtained glass after grinding it into a powder. The densified glass-ceramic samples were obtained by compressing the glass powders at 94 MPa and then heating at 280 °C or 300 °C for 2 h.

The electrical conductivities of the cold-pressed powder samples and the unified samples of the solid electrolytes were measured using an AC impedance method under Ar gas flow in the temperature range from −40 °C to 200 °C and from −40 °C to 280 °C, respectively. Impedance spectra were recorded using an impedance analyzer (Solartron, 1260) in the frequency range between 1 Hz and 5 MHz. The glass and glass-ceramic powders were pressed at 94 MPa into pellets with a 10 mm diameter in order to measure the conductivities in the cold-pressed state. Stainless steel plates were attached to both sides of the pellet as the electrodes. On the other hand, heat treatment to obtain the unified sample was carried out for a pellet of the glass powder with stainless steel plates on both faces as the electrodes. It was heated from room temperature to 280 °C or 300 °C, with a heating rate of 10 °C min^{-1}, and maintained at that temperature for 2 h for unification. Impedance measurements were then carried out. The morphologies of the solid electrolytes in the electrochemical cells for the impedance measurements were observed by scanning electron microscopy (JEOL, JSM6480LA).

The electrochemical stability of the obtained samples was evaluated by cyclic voltammetry. An electrochemical cell of the solid electrolyte was fabricated by placing ground solid electrolyte powder in a 10 mm diameter hole in an insulating tube and pressing it into a pellet. After the pellet was heated at 280 °C for 2 h for unification, a stainless-steel plate (area: 0.785 cm^2) and lithium foil were attached to the faces of the pellet as working and counter electrodes, respectively. A cyclic voltammogram was obtained using a potentio-/galvanostat (Solartron, 1286) at a scanning rate of 3 mV s^{-1} in the range from −0.1 to 5 V.

Notes and references

1 B. Scrosati, *Nature*, 1995, **373**, 557.

2 K. Takada, T. Inada, A. Kajiyama, H. Sasaki, S. Kondo, M. Watanabe, M. Murayama and R. Kanno, *Solid State Ionics*, 2003, **158**, 269.

3 Y. Seino, K. Takada, B.-C. Kim, L. Zhang, N. Ohta, H. Wada, M. Osada and T. Sasaki, *Solid State Ionics*, 2005, **176**, 2389.

4 R. Mercier, J.-P. Malugani, B. Fahys and G. Robert, *Solid State Ionics*, 1981, **5**, 663.

5 A. Pradel and M. Ribes, *Solid State Ionics*, 1986, **18–19**, 351.

6 J. H. Kennedy, *Mater. Chem. Phys.*, 1989, **23**, 29.

7 A. Hayashi, S. Hama, H. Morimoto, M. Tatsumisago and T. Minami, *J. Am. Ceram. Soc.*, 2001, **84**, 477.

8 K. Minami, A. Hayashi, S. Ujiie and M. Tatsumisago, *J. Power Sources*, 2009, **189**, 651.

9 R. Kanno and M. Murayama, *J. Electrochem. Soc.*, 2001, **148**, A742.

10 N. Kamaya, K. Homma, Y. Yamakawa, M. Hirayama, R. Kanno, M. Yonemura, T. Kamiyama, Y. Kato, S. Hama, K. Kawamoto and A. Mitsui, *Nat. Mater.*, 2011, **10**, 682.

11 H. Aono, E. Sugimoto, Y. Sadaoka, N. Imanaka and G. Adachi, *Solid State Ionics*, 1990, **40–41**, 38.

12 H. Aono, E. Sugimoto, Y. Sadaoka, N. Imanaka and G. Adachi, *Solid State Ionics*, 1991, **47**, 257.

13 Y. Inaguma, L. Chen, M. Itoh and T. Nakamura, *Solid State Ionics*, 1994, **70–71**, 196.

14 F. Mizuno, A. Hayashi, K. Tadanaga and M. Tatsumisago, *Adv. Mater.*, 2005, **17**, 918.

15 H. Yamane, M. Shibata, Y. Shimane, T. Junke, Y. Seino, S. Adams, K. Minami, A. Hayashi and M. Tatsumisago, *Solid State Ionics*, 2007, **178**, 1163.

16 F. Croce, A. D'Aprano, C. Nanjundiah, V. R. Koch, C. W. Walker and M. Salomon, *J. Electrochem. Soc.*, 1996, **143**, 154.

17 K. Hayamizu, Y. Aihara, S. Arai and M. Cirilo, *J. Phys. Chem. B*, 1999, **103**, 519.

This journal is © The Royal Society of Chemistry 2014

Energy Environ. Sci., 2014, **7**, 627–631 | **631**